ACS APPLIED MATERIALS & INTERFACES

Research Article

www.acsami.org

New Cu_3TeO_6 Ceramics: Phase Formation and Dielectric Properties

Xiaoli Zhu, Zhonghua Wang, Xinming Su, and Paula M. Vilarinho*

Department of Materials and Ceramics Engineering, Centre for Research in Ceramics and Composite Materials, CICECO, University of Aveiro, 3810-193 Aveiro, Portugal

ABSTRACT: Targeting low temperature cofired ceramics (LTCC) applications and base-metal electrode multilayer ceramic capacitors (BME-MLCCs), ceramics of a new composition, tricopper tellurate (Cu_3TeO_6), are reported here. The crystal structure of Cu_3TeO_6 was determined to be cubic, *Ia*3, with the unit cell parameter a = 9.538 Å. The sequence of phase formation is proposed with the oxidation of tetravalent tellurium (Te^{4+}) into hexavalent tellurium (Te^{6+}) as a key step for the formation of Cu_3TeO_6. Ceramics sintered at 865 °C with densities of 94% exhibit two dielectric anomalies in the temperature dependence of the dielectric response, around −150 °C and +50 °C, respectively, accompanied by obvious frequency dispersion of the relative permittivity (ε_r) and dielectric losses (tan δ), with an Arrhenius like behavior. A temperature stable dielectric region (near room temperature) formed between the two anomalies with $\varepsilon_r \sim 12$ and tan $\delta \sim 0.01$, and a very low positive temperature coefficient of the relative permittivity ($TC\varepsilon_r$), 2.07×10^{-4} °C^{-1}, was obtained in the same region. The low temperature dielectric anomaly is associated with the possible mixed Cu^+/Cu^{2+} valence in Cu_3TeO_6 ceramics, while the high temperature anomaly is attributed to point defect ordering, including V_O, $Cu_{Cu2+}^{+\prime}$, which might be formed during sintering. Therefore, Cu_3TeO_6 ceramics are of interest in view of not only the possible applications in BME-MLCCs, LTCC, and related technologies, but also for their possible compatibility with low cost abundant Cu electrodes.

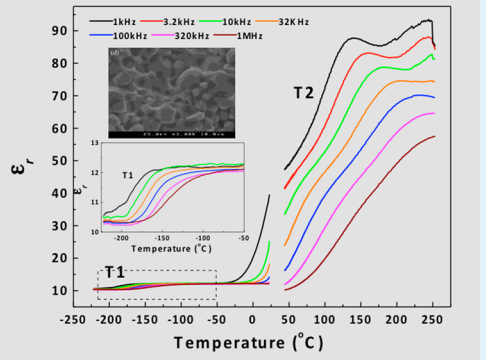

KEYWORDS: *copper tellurate, Cu_3TeO_6, phase formation, ceramics, dielectric characterization, low sintering temperature*

1. INTRODUCTION

With the rapid demand for microelectronics miniaturization and the development of wireless communications, the electronics industry needs to develop new, multifunctional, and miniaturized devices. By utilizing low-temperature cofired ceramics (LTCC) and base-metal electrode multilayer ceramic capacitors (BME-MLCCs) technology, passive components such as capacitors, inductors, and resistors can be easily integrated into chips. In these technologies, highly conductive silver metal is a common inner electrode because of its low conducting losses and cost. Therefore, cofiring temperature needs to be below 960 °C, which is the melting point of silver.

In the recent past, several Te-based compounds have been investigated as possible dielectric candidates for BME-MLCCs and LTCC applications due to their low synthesis and sintering temperature and good dielectric properties.[1−8] In contrast to glasses, the physical properties of Te-based ceramics have not been systematically explored. Suvorov and co-workers[1−5] have reported the phase formation and microwave dielectric properties of several Te-based compounds, such as Bi_2TeO_5 ($\varepsilon_r \sim 52$, $\tau_f \sim -49$ ppm/°C, sintered at 730 °C; ε_r being the relative permittivity and τ_f the temperature coefficient of resonance frequency),[1] $TiTe_3O_8$ ($\varepsilon_r \sim 50$, $\tau_f \sim 133$ ppm/°C, sintered at 720 °C),[2] and Bi_2TiTeO_8 ($\varepsilon_r \sim 36$, $\tau_f \sim 41$ ppm/°C, sintered at 840 °C).[3] Kwon and co-workers reported $BaTe_4O_9$ ceramics with an ε_r of 17.5 and τ_f of −90 ppm/°C sintered at 550 °C[6,7] and $BaTiTe_3O_9$ with an ε_r of 29 and τ_f of −372 ppm/°C sintered at 650 °C.[8] Moreover, $BaTe_4O_9$ ceramics were successfully cofired with aluminum electrodes, while maintaining good electrical performance. All of these Te-based ceramics can be well sintered below 900 °C, fulfilling the sintering conditions for application in LTCCs and BME-MLCCs.

However, research and relevant data on compounds of the $CuO\text{-}TeO_2$ system are rather scarce. Most of these limited studies covered structural, optical, and electrical properties of copper tellurium oxide glasses.[9] Earlier studies on the $CuO\text{-}TeO_2$ system were mainly focused on the determination of the crystallographic structures of compounds. So far, four compounds in the $CuO\text{-}TeO_2$ binary system, Cu_3TeO_6, $CuTe_2O_5$, $CuTeO_3$, and $CuTeO_4$, have been obtained from a solid-state reaction between the starting oxides and their crystal structures resolved. Cu_3TeO_6 has a cubic structure (*Ia*3), which is built up by TeO_6 octahedra connected through copper atoms. The crystal structure of Cu_3TeO_6 was calculated for the first time in 1968[10] and revised in 1978.[11] Lindqvist[12] and Hanke et al.[13] resolved the crystal structure of $CuTe_2O_5$ single crystals, grown based on the method described by Moret et al.[14] $CuTe_2O_5$ crystallizes with a monoclinic structure with the space group $P2_1/C$, and its unit cell parameters have been determined to be a = 6.871 Å, b = 9.322 Å, c = 7.602 Å, and θ = 109.08°.

Received: March 27, 2014
Accepted: June 24, 2014
Published: June 24, 2014

The structure is a three-dimensional network formed by copper and tellurium polyhedra sharing oxygen atoms. In $CuTeO_3$, there are two chemically different tellurium atoms in the structure, both of which are strongly bonded to three oxygen atoms, and the structure is orthorhombic with the unit cell parameters a = 7.604 Å, b = 12.705 Å, and c = 5.837 Å.[12,15] However, the space group of $CuTeO_3$ is not very consistent. Lindqvist et al. in two different publications reported the space group to be $P2_1nb$ or $Pmnb$[12] and $Pmcn$.[15] Later on, Gospodinov reported another binary copper tellurate compound, $CuTeO_4$, obtained by wet chemistry and processed between 267 and 470 °C,[16] which is quite unstable and decomposes into Cu_3TeO_6 + TeO_2 + O_2 at 595 °C in the air, while in an inert medium this decomposition occurs at 510 °C. The crystal structure of $CuTeO_4$ was reported by Falck et al.[17] as orthorhombic $P2_1/n$ with the lattice parameters a = 5.500(2) Å, b = 10.327(7) Å, c = 4.704(2) Å, and Z = 4.

According to these previous reports, Cu_3TeO_6 is the most stable composition in the CuO-TeO_2 system. However, the phase formation process of Cu_3TeO_6 is not yet clear. In addition, no systematic studies on the ceramic fabrication and electrical properties of Cu_3TeO_6 have been reported. Only magnetic properties of single crystals of Cu_3TeO_6 have been recently reported by Herak et al.[18,19] The magnetic susceptibility of Cu_3TeO_6 in the paramagnetic state obeys the Curie–Weiss law in the 200–330 K range with Θ_{CW} (Curie–Weiss temperature) = −148 K and at T_N (Neel temperature) = 61 K, the system undergoing an antiferromagnetic phase transition. The existence of antiferromagnetic behavior makes the study of electrical properties in Cu_3TeO_6 even more interesting. Moreover, Cu is an attractive potential electrode in microelectronics due to its low cost and high conductivity. Therefore, the fabrication of Cu_3TeO_6 ceramics and the characterization of electrical properties are of interest not only in view of the possible applications in BME-MLCCs, LTCC, and related technologies but also for the possible compatibility with Cu electrodes.

In the present work, Cu_3TeO_6 powders and ceramics are fabricated by conventional solid-state reaction and sintering. The phase formation sequence, structure, and microstructure are investigated and the dielectric properties reported.

2. EXPERIMENTAL SECTION

Cu_3TeO_6 powders were synthesized by conventional solid-state reactions, using reagent-grade copper oxide (CuO, British Drug Houses Ltd., purity >99%) and tellurium dioxide (TeO_2, Sigma-Aldrich, purity >99%) powders as the raw materials, according to the molar ratio $3CuO/1TeO_2$. The weighed raw materials were loaded together with ethanol into Teflon containers and mixed in a planetary ball miller for 24 h at a constant speed of 200 rpm. After drying at 60 °C for 10 h, the mixture was calcined in high-purity alumina crucibles at temperatures ranging from 400 to 750 °C for 5 h, in the air. Thermogravimetric analysis (TG) and differential thermal analysis (DTA; SETARAM Labsys TG-DTA12) of copper oxide and tellurium dioxide powders were conducted to study the phase formation process. These studies were supported by *in situ* high-temperature XRD (Philips X'-Pert, Cu$K\alpha$) used to follow *in situ* the phase formation as a function of temperature. The Pt peak in the *in situ* patterns corresponds to the platinum crucible used in these experiments. The heating rate was kept at 10 °C/min. Calcined and ball milled Cu_3TeO_6 powders were used to prepare bulk ceramics. Dried powders were uniaxially pressed at 25 MPa (Carver Laboratory Press, Fred S. Carver Inc., USA) into disks of 10 mm diameter and 4 mm thickness, then submitted to Cold Isostatic Pressing (CIP; Stansted Fluid Power Ltd.) at 200 MPa. Sintering was performed at temperatures ranging from 750 to 900 °C. Due to the high volatility of tellurium dioxide, ceramics were sintered in closed alumina crucibles with small amounts of TeO_2 powders. The density of the sintered samples was measured with the Archimedes method and was around 94% of the theoretical density.

X-ray diffraction (XRD) analyses, using a Rigaku Geiger flex D/Max-B (Tokyo, Japan) and Cu Kα radiation, were performed to inspect the formed phases. Microstructures of Cu_3TeO_6 ceramics were observed with scanning electron microscopy (SEM, Hitachi S-4100). For the electrical measurements, 6 mm diameter gold electrodes were deposited through a shadow mask onto the surfaces of the ceramics. After the deposition, ceramic disks were annealed at 80 °C for 20 min to improve the gold/ceramic interface. Relative permittivity and loss tangent of Cu_3TeO_6 ceramics were measured with a precision LCR meter (4284A, Hewllet Packard) from room temperature (~25 °C) to 250 °C over a frequency ranging from 1 kHz to 1 MHz. Low temperature dielectric properties were collected over a frequency range of 100 Hz to 1 MHz and from room temperature cooling to 10 K using a homemade system with an Agilent E4980A Precision LCR meter (Santa Clara, CA, USA) and closed cycle helium cryostat (ARS-2HW Compressor, Advanced Research Systems, Inc., Macungie, PA, USA).

3. RESULTS AND DISCUSSION

3.1. Phase Formation of Cu_3TeO_6. Monophasic Cu_3TeO_6 was obtained with the conventional solid state reaction method, calcined at temperatures ranging from 550 to 700 °C for 5 h. X-ray diffraction patterns of $3CuO+TeO_2$ powders calcined at 650 °C are shown in Figure 1. All of the peaks are indexed

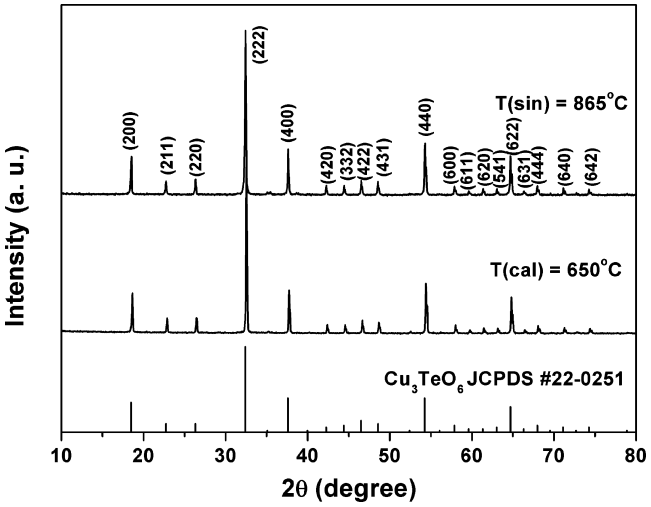

Figure 1. X-ray diffraction patterns of Cu_3TeO_6 powders calcined at 650 °C and ceramics sintered at 865 °C. Cu_3TeO_6 powders and ceramics are monophasic.

according to the JCPDS card #22-0251. The crystal structure of Cu_3TeO_6 was determined to be cubic, $Ia3$ with a unit cell parameter of a = 9.538 Å, in accordance with the results reported by Hostachy and Coing-Boyat.[10]

Figure 2 presents the thermogravimetric analysis (TG) and differential thermal analysis (DTA) data of the $3CuO+TeO_2$ mixture. As clearly seen in the TG curve (Figure 2a), there is a weight increase that begins at about 450 °C, accelerating obviously at temperatures higher than 550 °C and attaining a maximum value at 650 °C with an overall weight gain of 3.83%. The DTA curve presents several thermal effects: a small exothermic peak around 200 °C, a quite strong exothermic one at ~450 °C after a very weak endothermic tendency, a sharp endothermic peak followed by an intense exothermic one

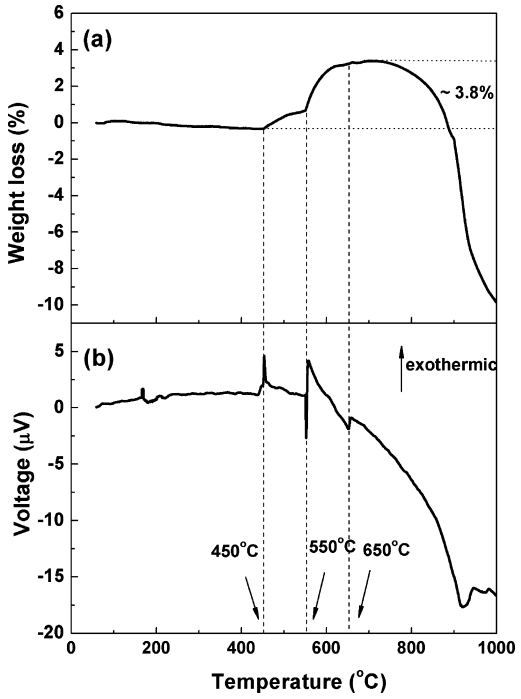

Figure 2. Thermogravimetric (a) and differential thermal analysis data (b) of the composition $3CuO+TeO_2$. The formation of Cu_3TeO_6 starts at 450 °C and is completed at 650 °C.

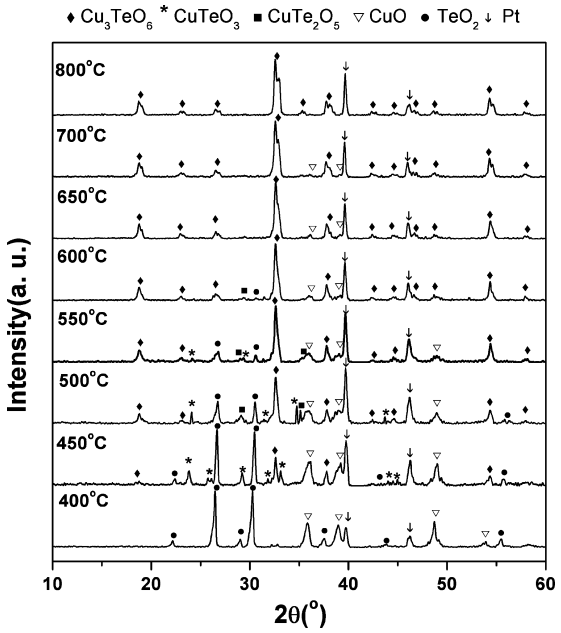

Figure 3. In situ XRD of CuO and TeO_2 (3:1) as a function of the temperature in the air. The Pt peak corresponds to the platinum crucible used in the experiments. In the air, the formation of Cu_3TeO_6 starts at 450 °C and is completed at 650 °C.

around 550 °C, and an endothermic peak at ~650 °C. It seems that all the thermal effects appear as endothermic and exothermic peak pairs with the endothermic a little bit before the exothermic one. Only the exothermic effect around 650 °C is too weak to identify.

Not considering intermediate reactions, the overall chemical reaction for the formation of Cu_3TeO_6 starting from the $3CuO+TeO_2$ mixture could be written as

$$3CuO + TeO_2 + 1/2O_2 \rightarrow Cu_3TeO_6$$

And accordingly, the theoretical associated weight gain is calculated to be 3.86%, which is in a good agreement with our thermogravimetric results; this observation allows us to relate this weight increase with the intake of oxygen.

To clarify the phase formation process in the $3CuO:1TeO_2$ system, in situ XRD analyses with increasing temperature were carried out from room temperature up to 800 °C in the air. No phase change was observed at temperatures below 400 °C, and the in situ XRD patterns are presented in Figure 3 from 400 to 800 °C. Therefore, the small exothermic peak around 200 °C is not related with the reaction between CuO and TeO_2 and could be attributed to the burning of some residual organics, left from the powder processing. At 400 °C, only CuO and TeO_2 phases can be identified, indicating that there is no reaction up to this temperature. CuO and TeO_2 start reacting at 450 °C, where two new phases can be identified: $CuTeO_3$, present in high content and Cu_3TeO_6, as a minor one, besides CuO and TeO_2. Therefore, two kinds of reactions occurred: the oxidation of Te^{4+} to Te^{6+} and the synthesis reactions of CuO + TeO_2 to $CuTeO_3$ and of 3CuO + TeO_3 to Cu_3TeO_6. The oxidation of TeO_2 is endothermic.[25,26] Hence the exothermic peak at 450 °C in the DTA is suggested to be related mainly to the formation of $CuTeO_3$, and the weak endothermic tendency corresponds to the start of the oxidation from Te^{4+} to Te^{6+}. The appearance of a Cu_3TeO_6 minor phase at 450 °C explains the start of the weight increase at the same temperature in the TG curve.

As the temperature increases from 500 to 600 °C, the reaction between CuO and TeO_2 continues, and three products are detected: $CuTeO_3$, $CuTe_2O_5$, and Cu_3TeO_6, while peaks of the two oxide precursors decrease in intensity. In agreement with the phase diagram of Ivanova et al.,[20] $CuTeO_3$ and $CuTe_2O_5$ are the two stable compounds detected in the CuO-TeO_2 system, and the eutectic point is at 615 °C. Therefore, the presence of these two phases in this temperature range is very reasonable. Meanwhile, the increase of the peak intensity of the Cu_3TeO_6 phase indicates the continued oxidation of Te^{4+} in $CuTeO_3$, $CuTe_2O_5$, and TeO_2 into Te^{6+} and corresponds to the weight increase in this temperature range observed in the TG curve. At 550 °C, the XRD peak of the Cu_3TeO_6 phase becomes the strongest peak, indicating the accelerated phase formation, which coincides with the slope increase in the TG curve at the same temperature. The sharp endothermic and the strong exothermic DTA peaks around 550 °C are attributed to the rapid oxidation from Te^{4+} to Te^{6+} and formation of $CuTeO_3$, $CuTe_2O_5$, and Cu_3TeO_6, respectively. Hence, 550 °C is the low temperature limit to get monophasic Cu_3TeO_6. Above 650 °C, all of the peaks of the cubic Cu_3TeO_6 phase can be identified. Only a small amount of CuO is detected, which may be related with the volatility of TeO_2. The endothermic DTA peak around 650 °C is attributed to the oxidation of the rest of TeO_2.

Indeed, the oxidation of TeO_2 has been reported in several works.[21−27] Similar observations have been reported by Dimitriev et al.[25] in the $1CuO:1TeO_2$ system. In spite of the different stoichiometries of 1:1 versus 3:1, a very similar TG profile was reported in their work, with an increase of the mass beginning at about 450−460 °C and attaining a maximum value at 650 °C, as in our case. The authors attributed this variation to the oxidation of Te^{4+} to Te^{6+}. Above 870 °C, an opposite effect was found, namely a decrease of the mass attributed to

the dissociation and melting of Cu−Te compounds, also in accordance with the results of the present study. More recently, and related to phase formation in the Al_2O_3−TeO_2 system, we reported that TeO_2 oxidation accompanied by a weight increase of around 3% occurs in the air at >600 °C to form Te_4O_9 and TeO_3, and it triggers the formation of Al_2TeO_6.[26] In 1CuO:1TeO_2 systems, the higher reactivity of CuO forces the oxidation of Te^{4+} at much lower temperatures than in the case of the Al_2O_3:TeO_2 system.

Therefore, we propose that the sequence of reaction of phase formation in 3CuO:TeO_2 in the air is

$$3CuO + TeO_2 + \frac{1}{2}O_2 \rightarrow Cu_3TeO_6 \quad (450\ ^\circ C < T < 650\ ^\circ C) \tag{1}$$

$$CuO + TeO_2 \leftrightarrow CuTeO_3\ (T \sim 450\ ^\circ C) \tag{2}$$

$$CuTeO_3 + 2CuO + \frac{1}{2}O_2 \rightarrow Cu_3TeO_6 \quad (450\ ^\circ C < T < 650\ ^\circ C) \tag{3}$$

$$CuO + 2TeO_2 \leftrightarrow CuTe_2O_5\ (T \sim 500\ ^\circ C) \tag{4}$$

$$CuTe_2O_5 + 5CuO + O_2 \rightarrow 2Cu_3TeO_6 \quad (500\ ^\circ C < T < 650\ ^\circ C) \tag{5}$$

$$TeO_2 + O_2 \rightarrow TeO_3\ (T \sim 650\ ^\circ C) \tag{6}$$

$$3CuO + TeO_3 \rightarrow Cu_3TeO_6\ (T \sim 650\ ^\circ C) \tag{7}$$

3.2. Cu_3TeO_6 Bulk Ceramics. *3.2.1. Sintering Properties.* The sintering behavior of Cu_3TeO_6 powders was assessed by plotting the volume shrinkage and relative densities of the ceramics versus sintering temperatures, as shown in Figure 4.

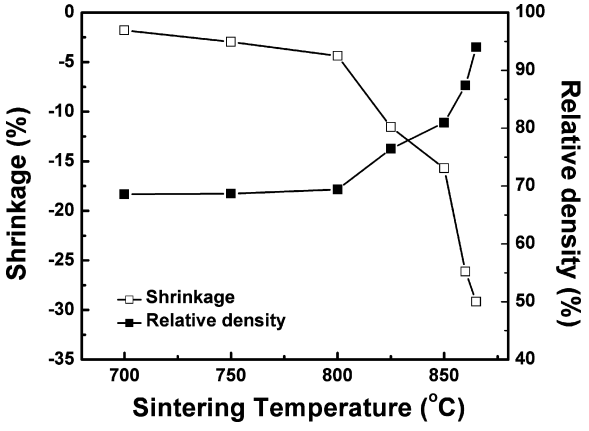

Figure 4. Variation of volumetric shrinkage and relative density of Cu_3TeO_6 ceramics with the sintering temperature. Dense ceramics with a relative density of 94% can be obtained at 865 °C.

The densification of Cu_3TeO_6 ceramics starts at temperatures between 800 and 820 °C. For temperatures higher than 850 °C, the shrinkage and the relative density change rapidly. At temperatures above 870 °C, the warpage of the sintered sample is so significant that it is no longer possible to accurately determine the volume shrinkage of the specimen. Quite dense ceramics were obtained after sintering at 865 °C, with a relative density of 94% and shrinkage of ∼30%.

Cu_3TeO_6 ceramics sintered at various temperatures were characterized by XRD analysis to assess the compositional stability. Tellurium (Te) has high vapor pressure, so it is likely to vaporize at even moderate temperatures, especially when the partial pressure of Te in the atmosphere is lower than that in the ceramic bulk. In order to prevent the volatilization of Te, the ceramic disks were sintered in a closed crucible and surrounded by TeO_2 powder. The XRD pattern for ceramics sintered at 865 °C is also shown in Figure 1. The composition of Cu_3TeO_6 ceramics sintered at different temperatures is identical to that of the green body. No decomposition of the Cu_3TeO_6 phase is observed at these temperatures. Therefore, Cu_3TeO_6 is stable at and below 865 °C, under these sintering conditions.

The microstructure of Cu_3TeO_6 ceramics sintered at different temperatures was assessed by SEM. The micrographs of the fracture surface of these ceramics are illustrated in Figure 5. For ceramics sintered at 750 °C (Figure 5a), no significant grain growth was observed, and the particles still appeared as discrete ones. Most of the grains show a diameter of less than 3.5 μm, and the large particles remain with the plate-like shape that characterizes the calcined powders. At this temperature, the volumetric shrinkage and relative density are 2.96% and 68.67%, respectively. A gradual grain growth was observed after sintering at 850 and 860 °C (Figure 5b,c). The grains have mainly a dodecahedron shape, characteristic of a final stage of densification. A relative density higher than 89% was achieved after sintering at 860 °C. The micrograph of the ceramics sintered at 865 °C (Figure 5d) indicates the existence of a liquid phase during the sintering process, which helps the densification. The resultant ceramic has a relative density of 94% and a volumetric shrinkage of 29%.

3.2.2. Dielectric Characteristics. Figure 6 illustrates the relative permittivity (ε_r) and dielectric loss (tan δ) as a function of the temperature measured at different frequencies for Cu_3TeO_6 ceramics sintered at 865 °C. Relative permittivity of Cu_3TeO_6 increases from 10 to 50 after two dielectric anomalies (denoted as T1 and T2 in Figure 6) with increasing temperature in the frequency range of 1 kHz to 1 MHz. The first of the two dielectric anomalies appears at around −150 °C, with one increase of ε_r from 10 to 12, accompanied by obvious frequency dispersion of ε_r and tan δ. The second one appears at around +50 °C, and a similar frequency dispersion in ε_r and tan δ is also observed. A temperature stable dielectric region forms between the above two anomalies with the ε_r ∼12 and tan δ ∼0.01 in the temperature range from −100 to 12 °C at 1 MHz.

The corresponding variations of the maximum temperature (T_m) with frequency observed in both sets of tan δ peaks obey the Arrhenius law:

$$f = f_0 \exp(-E_a/kT_m)$$

where f_0 is the pre-exponential term, E_a is the activation energy, and k is the Boltzmann constant. The obtained fitting parameters are E_a = 0.06 eV and $f_0 = 6.14 \times 10^8$ Hz for the first anomaly and E_a = 0.5 eV and $f_0 = 4.75 \times 10^{12}$ Hz for the second one. The ln $f \sim 1/T_m$ relationship and the Arrhenius fitting are represented in Figure 7. The results of the Arrhenius fitting indicate these two dielectric anomalies as thermally activated processes.

The dielectric behavior observed here for Cu_3TeO_6 ceramics is quite similar to that of other dielectric systems, like $CaCu_3Ti_4O_{12}$,[28] and some others with Fe ion substitution, such as $Ba(Fe_{1/2}B_{1/2})O_3$ (B = Nb, Ta)[29,30] and

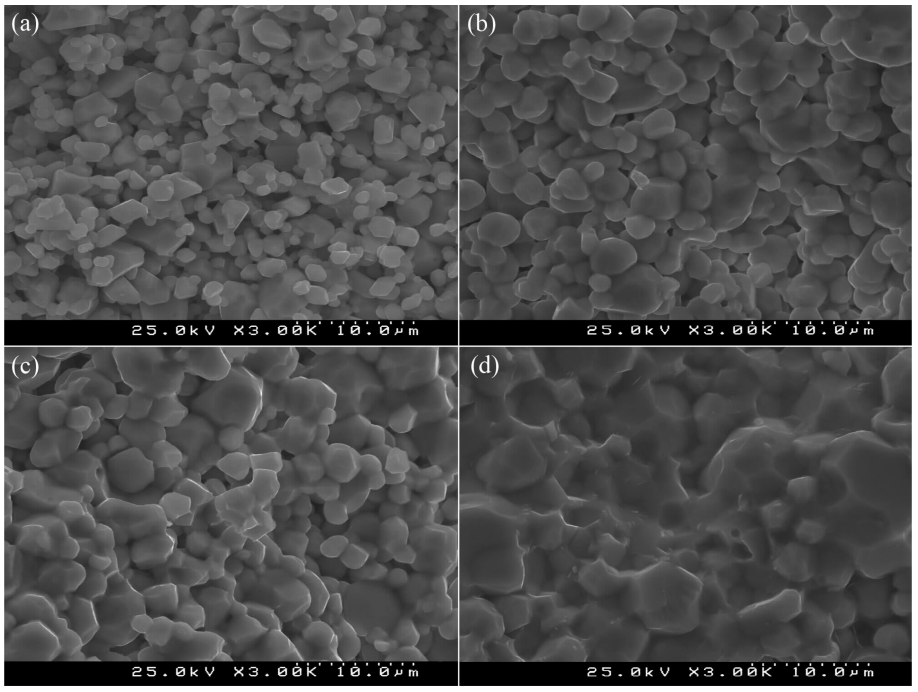

Figure 5. Fracture surface micrographs of Cu_3TeO_6 ceramics sintered at 750 °C (a), 850 °C (b), 860 °C (c), and 865 °C (d). Cu_3TeO_6 ceramics present dense microstructures with grain size increasing with increasing sintering temperature.

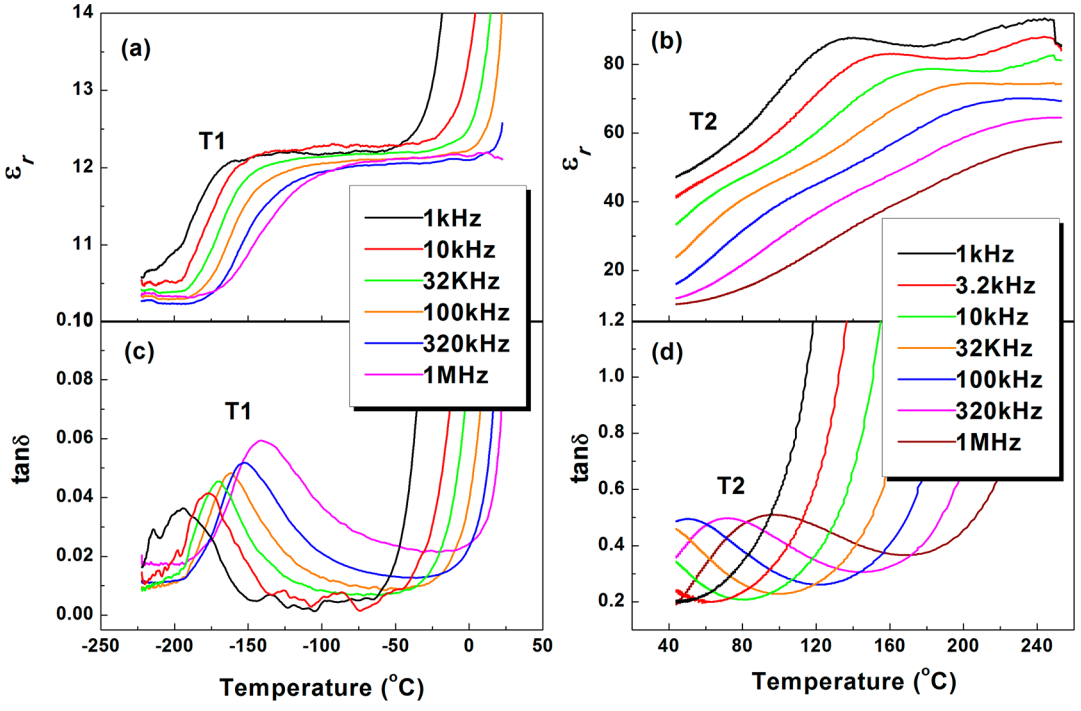

Figure 6. Temperature and frequency dependences of relative permittivity (a and b) and dielectric loss (c and d) for Cu_3TeO_6 ceramics sintered at 865 °C in the temperature range of −225 °C to +260 °C, and frequencies from 1 kHz to 1 MHz. Two dielectric anomalies are visible, denoted as T1 and T2.

$Ba_5NdFe_{1.5}Nb_{8.5}O_{30}$,[31] where a temperature-stable dielectric constant step forms between two relaxation-like dielectric anomalies. As in the present case, the dielectric anomalies in all of these compositions obey the Arrhenius law. The fitting parameters are listed in Table 1 for comparison. Generally, the low temperature anomaly has a small activation energy with a characteristic frequency $f_0 \sim 10^8$. In $CaCu_3Ti_4O_{12}$, this behavior has been attributed to the mixed valence structure, arising from the mixed-valence Cu^+/Cu^{2+} and Ti^{3+}/Ti^{4+} that creates dipoles in the structure that relax with temperature and frequency;[28] while in Fe-based compositions, the low temperature anomaly is considered as a nearly Debye relaxation, originated from the dipole effects associated with the charge carrier hopping between Fe^{2+} and Fe^{3+} inside the grains.[29−31] Therefore, and by analogy, the low temperature anomaly in Cu_3TeO_6 may be related to the possible mixed Cu^+/Cu^{2+}valence in Cu_3TeO_6

dx.doi.org/10.1021/am501742z | ACS Appl. Mater. Interfaces 2014, 6, 11326−11332

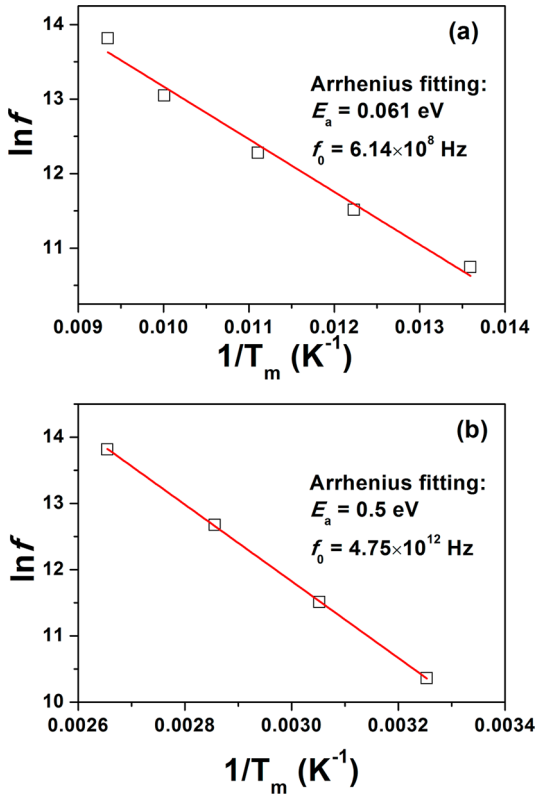

Figure 7. ln $f \sim 1/T_m$ relationship (open square) and the Arrhenius fittings (red line) for the two dielectric anomalies: T1 (a) and T2 (b), respectively.

ceramics. Regarding the high temperature anomaly, Cu_3TeO_6 has comparable E_a and f_0 values to $CaCu_3Ti_4O_{12}$ as well, being attributed to the results of possible point defect ordering, including V_O, $Cu^{+\prime}{}_{Cu2+}$, which is generally formed during sintering in the air. Moreover, the magnitude of the dielectric constant step depends on the intrinsic polarizability of the material system. For $CaCu_3Ti_4O_{12}$ and $Ba(Fe_{1/2}B_{1/2})O_3$ ceramics with giant relative permittivity, the permittivity step can reach 10^4,[28−30] while it is around 10^3 in $Ba_5NdFe_{1.5}Nb_{8.5}O_{30}$.[31] For the case of Cu_3TeO_6, the much lower relative permittivity justifies the small magnitude of the observed step between the two dielectric peaks. Indeed, Te-based materials have comparably quite low relative permittivity, such as in Bi_2TeO_5 ($\varepsilon_r \sim 52$),[1] $TiTe_3O_8$ ($\varepsilon_r \sim 50$),[2] Bi_2TiTeO_8($\varepsilon_r \sim 36$),[3] $BaTe_4O_9$ (ε_r ~17.5),[6,7] and $BaTiTe_3O_9$ (ε_r ~29),[8] that reflects the low polarizability of Te ions.

The temperature coefficient of the relative permittivity ($TC\varepsilon_r$) is calculated by the relation: $TC\varepsilon_r = \Delta\varepsilon_r/\varepsilon_0\Delta T$, where $\Delta\varepsilon_r$ stands for the change in relative permittivity within the temperature range between the two dielectric anomalies, from −100 to 12 °C for 1 MHz, and ε_0 for the permittivity at −100 °C. Between the two dielectric anomalies, the temperature coefficients of relative permittivity of dense Cu_3TeO_6 ceramics exhibit a very low positive value of about 2.07×10^{-4} °C^{1-}.

4. CONCLUSIONS

Monophasic Cu_3TeO_6 was obtained through conventional solid state reaction, calcined at temperatures ranging from 550 to 700 °C. The crystal structure of Cu_3TeO_6 was determined to be cubic, *Ia*3 with the unit cell parameter a = 9.538 Å. The phase formation mechanism of Cu_3TeO_6 was investigated. It is proposed that the formation of Cu_3TeO_6 starts at 450 °C. The weight gain of 3.83% detected by thermogravimetric analysis coincides with the weight increase associated with Te oxidation during Cu_3TeO_6 phase formation. It is proposed that the oxidation of tetravalent tellurium (Te^{4+}) into hexavalent tellurium (Te^{6+}) is a key step for the formation of Cu_3TeO_6. Dense ceramics were obtained after sintering at 865 °C with a relative density of 94%. Very interestingly from the point of view of applications, these ceramics exhibit a temperature stable dielectric region formed between the two anomalies, near room temperature (> −150 °C and < +150 °C), with $\varepsilon_r \sim 12$, low dielectric losses ($\tan\delta \sim 0.01$), and a $TC\varepsilon_r = 2.07 \times 10^{-4}$ °C^{-1}. The two dielectric anomalies were well fitted to the Arrhenius law, and the activation energy for the dispersion process calculated. The low temperature anomaly was associated with the possible mixed Cu^+/Cu^{2+} valence in Cu_3TeO_6 ceramics, while the high temperature anomaly was attributed to the results of point defect ordering, including V_O, $Cu^{+\prime}{}_{Cu2+}$, which are generally formed during sintering in the air. The plateau in which the dielectric permittivity and losses are quite stable makes these materials interesting candidates for stable dielectric permittivity applications. In addition, the low temperature required to sinter Cu_3TeO_6 ceramics, the predicted compatibility with possible low cost Cu electrodes, and a magnetic response allows us to consider Cu_3TeO_6 ceramics as promising electroceramics with possible coupled functionalities.

AUTHOR INFORMATION

Corresponding Author

*E-mail: paula.vilarinho@ua.pt.

Notes

The authors declare no competing financial interest.

ACKNOWLEDGMENTS

The authors acknowledge Fundação para a Ciência e a Tecnologia (FCT), Fundo Europeu de Desenvolvimento Regional Portugal (FEDER), QREN-COMPETE Portugal, and the Associate Laboratory CICECO (PEst-C/CTM/LA0011/2013) for funding support. X.S. and X.Z. acknowledge FCT for financial support (SFRH/BD/44311/2008 and

Table 1. Characteristic Parameters of the Two Dielectric Anomalies in Different Compositions

composition	anomaly 1 (low T)			anomaly 2 (high T)			ref
	T_m (°C)	E_a (eV)	f_0(Hz)	T_m (°C)	E_a (eV)	f_0 (Hz)	
Cu_3TeO_6	−190 to −150	0.06	6.14×10^8	50−100	0.5	4.75×10^{12}	this work
$CaCu_3Ti_4O_{12}$	−150 to −110	0.156	0.94×10^8	50−230	0.515	0.8×10^{11}	28
$Ba(Fe_{1/2}Nb_{1/2})O_3$	−20 to 100	0.174	0.23×10^8	>200	0.83	0.3×10^4	29
$Ba(Fe_{1/2}Ta_{1/2})O_3$	−20 to 100	0.176	0.18×10^8	>200	0.797	0.3×10^3	30
$Ba_5NdFe_{1.5}Nb_{8.5}O_{30}$	0−100	0.19	1.3×10^8	>200			31

SFRH/BPD/82534/2011). Thanks to Rob C. Pullar for proofreading the English in this article.

REFERENCES

(1) Udovic, M.; Valant, M.; Suvorov, D. Characterization of the Bi_2O_3-TeO_2 System with Respect to Oxygen Partial Pressure Key. *Eng. Mater.* **2002**, *206*, 1409−1412.
(2) Udovic, M.; Valant, M.; Suvorov, D. Dielectric Characterization of Ceramics from the TiO_2-TeO_2 System. *J. Eur. Ceram. Soc.* **2001**, *21*, 1735−1738.
(3) Udovic, M.; Suvorov, D. Sintering and Dielectric Characterization of Pseudo Ternary Compounds from the Bi_2O_3−TiO_2−TeO_2 System. *J. Am. Ceram. Soc.* **2007**, *90*, 2404−2408.
(4) Udovic, M.; Valant, M.; Jancar, B.; Suvorov, D. Phase Formation and Crystal-Structure Determination in the Bi_2O_3-TiO_2-TeO_2 System Prepared in an Oxygen Atmosphere. *J. Am. Ceram. Soc.* **2006**, *89*, 3462−3469.
(5) Valant, M.; Suvorov, D. Glass-Free Low-Temperature Cofired Ceramics: Calcium Germinates, Silicates and Tellurates. *J. Eur. Ceram. Soc.* **2004**, *24*, 1715−1719.
(6) Kwon, D.; Lanagan, M.; Shrout, T. Microwave Dielectric Properties and Low-temperature Cofiring of $BaTe_4O_9$ with Aluminum Metal Electrode. *J. Am. Ceram. Soc.* **2005**, *88*, 3419−3422.
(7) Kwon, D.; Lanagan, M.; Shrout, T. Microwave Dielectric Properties of BaO-TeO_2 Binary Compounds. *Mater. Lett.* **2007**, *61*, 1827−1831.
(8) Kwon, D.; Lanagan, M.; Shrout, T. Synthesis of $BaTiTe_3O_9$ Ceramics for LTCC Application and Its Dielectric Properties. *J. Ceram. Soc. Jpn.* **2005**, *113*, 216−219.
(9) Hassan, M.; Hogarth, C. A study of Structural, Electrical and Optical Properties of Copper Tellurium Oxide Glasses. *J. Mater. Sci.* **1988**, *23*, 2500−2504.
(10) Hostachy, A.; Coing-Boyat, J. Structure Crystalline de Cu_3TeO_6. *Acad. Sci. (Paris)* **1968**, *B267*, 1435−1438.
(11) Falck, L.; Lindqvist, O.; Moret, J. Tricopper Tellurate. *Acta Crystallogr.* **1978**, *B34*, 896−897.
(12) Lindqvist, O. On the Structures of $CuTeO_3$ and $CuTe_2O_5$. *Acta Chem. Scand.* **1971**, *25*, 740.
(13) Hanke, K.; Kupcik, V.; Lindqvist, O. The Crystal Structure of $CuTe_2O_5$. *Acta Crystallogr.* **1973**, *B29*, 963−970.
(14) Moret, J.; Philippo, E.; Maurin, M. Structural Study of 2 New Crystalline Phases TeO_2, CuO-2TeO_2, CuO. *C. R. (Dokl.) Acad. Sci. URSS* **1969**, *C269*, 123−125.
(15) Lindqvist, O. The Crystal Structure of $CuTeO_3$. *Acta Chem. Scand.* **1972**, *26*, 1423−1430.
(16) Gospodinov, G. Phase States of Copper Orthotellurates in an Aqueous Medium and in Thermolysis. *J. Mater. Sci. Lett.* **1992**, *11*, 1460−1462.
(17) Falck, L.; Lindqvist, O.; Mark, W. The Crystal Structure of $CuTeO_4$. *Acta Crystallogr.* **1978**, *B34*, 1450−1453.
(18) Herak, M.; Berger, H.; Prester, M.; Miljak, M.; Živković, I.; Milat, O.; Drobac, D.; Popovićand, S.; Zaharko, O. Novel Spin Lattice in Cu_3TeO_6: an Antiferromagnetic Order and Domain Dynamics. *J. Phys.: Condens. Matter* **2005**, *17*, 7667−7679.
(19) Herak, M. Cubic Magnetic Anisotropy of the Antiferromagnetically Ordered Cu_3TeO_6. *Solid State Commun.* **2011**, *151*, 1588−1592.
(20) Ivanova, I.; Marinov, M.; Dimitriev, I. B. Phase Diagram and Electrical Properties in the Copper(II) Oxide-Tellurium(IV) Oxide System. *Dokl. Bolg. Akad. Nauk* **1972**, *25*, 1391−1394.
(21) Frit, B.; Jaymes, M.; Perez, G.; Hagenmuller, P. Binary System Bi_2O_3-TeO_2 at 750 °C. *Rev. Chim. Miner.* **1971**, *8*, 453.
(22) Takeshi, K.; Yoshizo, K.; Masato, Y.; Hiroshi, S. Pseudo-Binary System Bi_2O_3-TeO_2 in Air. *J. Mater. Sci.* **1989**, *24*, 4275−4278.
(23) Thomas, P.; Jeansannetas, B.; Champarnaud-Mesjard, J.; Frit, B. Crystal Structure of a New Mixed-valence Bismuth Oxotellurate (Bi_2TeTeO_8)-Te-IV-Te-VI. *Eur. J. Solid State Inorg. Chem.* **1996**, *33*, 637−646.
(24) Udovic, M.; Valant, M.; Suvorov, D. Formation and Decomposition of the Bi_2TeO_6 Compound. *J. Eur. Ceram. Soc.* **2004**, *24*, 953−958.
(25) Dimitriev, Y.; Gatev, E.; Ivanova, Y. High-temperature X-Ray Study of the Oxidation of $CuTeO_3$. *J. Mater. Sci. Lett.* **1989**, *8*, 230−231.
(26) Su, X.; Wu, A.; Vilarinho, P. Al_2TeO_6: Mechanism of Phase Formation and Dielectric Properties. *Scr. Mater.* **2012**, *67*, 927−930.
(27) Bayer, G. Zur Kristallchemie des Tellurs. *Fortschr. Mineral., Beih.* **1969**, *46*, 42−72.
(28) Ni, L.; Chen, X. Dielectric Relaxations and Formation Mechanism of Giant Dielectric Constant Step in $CaCu_3Ti_4O_{12}$ Ceramics. *Appl. Phys. Lett.* **2007**, *91*, 122905.
(29) Wang, Z.; Chen, X. M.; Ni, L.; Liu, X. Q. Dielectric Abnormities of Complex Perovskite $Ba(Fe_{1/2}Nb_{1/2})O_3$ Ceramics Over Broad Temperature and Frequency Range. *Appl. Phys. Lett.* **2007**, *90*, 022904.
(30) Wang, Z.; Chen, X. M.; Ni, L.; Liu, Y. Y.; Liu, X. Q. Dielectric Relaxations in $Ba(Fe_{1/2}Ta_{1/2})O_3$ Giant Dielectric Constant Ceramics. *Appl. Phys. Lett.* **2007**, *90*, 102905.
(31) Bai, Y.; Zhu, X. L.; Chen, X. M.; Liu, X. Q. Dielectric and Ferroelectric Characteristics of $Ba_5NdFe_{1.5}Nb_{8.5}O_{30}$ Tungsten Bronze Ceramics. *J. Am. Ceram. Soc.* **2010**, *93*, 3573−3576.